



Unclassified

SECURITY CLASSIFICATION OF THIS PAGE

## REPORT DOCUMENTATION PAGE

1a REPORT SECURITY CLASSIFICATION  
Unclassified

ELECTE

1b RESTRICTIVE MARKINGS

2a SECURITY CLASSIFICATION

MAR 27 1980

3 DISTRIBUTION/AVAILABILITY OF REPORT

EDULE

unlimited

IMBRE

5. MONITORING ORGANIZATION REPORT NUMBER(S)

AFOSR-TN-89-0315

AD-A205 713

6a. NAME OF PERFORMING ORGANIZATION  
Dept. of Aerospace Engineering6b. OFFICE SYMBOL  
*(If applicable)*

7a. NAME OF MONITORING ORGANIZATION

6c. ADDRESS (City, State and ZIP Code)  
Texas A&M University  
College Station, TX 77843-3141

7b. ADDRESS (City, State and ZIP Code)

Bolling Air Force Base  
Washington, D.C. 203328a. NAME OF FUNDING  
ORGANIZATION

ONSORING

8b. OFFICE SYMBOL  
*(If applicable)*

9. PROCUREMENT INSTRUMENT IDENTIFICATION NUMBER

DASC/SL

Grant No. AFOSR-84-0066

6c. ADDRESS (City, State and ZIP Code)

DASC/SL 713

10. SOURCE OF FUNDING NO.

PROGRAM ELEMENT NO.	PROJECT NO.	TASK NO.	WORK UN. NO.
61103F	2341	132	

11. TITLE (Include Security Classification)

Ultrasonic Nondestructive Evaluation of Damage in Continuous Fiber Composites

12. PERSONAL AUTHORITY

Vikram K. Kinra

13a. TYPE OF REPORT  
FINAL

13b. TIME COVERED

FROM 02/01/84 TO 12/31/87

14. DATE OF REPORT (YR., MO., DAY)

November 1987

15. PAGE COUNT

16. SUPPLEMENTARY NOTATION

## 17. COSATI CODES

FIELD	GROUP	SUB. GR.

## 18. SUBJECT TERMS (Continue on reverse if necessary and identify by block numbers)

Composites, Damage  
Velocity Attenuation  
Ultrasonic Nondestructive Evaluation

19. ABSTRACT (Continue on reverse if necessary and identify by block numbers)

It is well-known that composite materials develop a complex damage state when they are subjected to monotonic or fatigue loading. The damage has, in general, two effects on the propagation of an ultrasonic wave: it decreases the stiffness and increases the attenuation. The central objective of this work has been to correlate damage states with changes in the two ultrasonic parameters (wavespeed and attenuation).

We have developed a new technique for measuring the wavespeed and attenuation in the thickness direction, in extremely thin laminates. We have also developed a technique for the excitation and detection of Lamb waves in the lengthwise direction. Thus, both the in-plane and out-of-plane measurements can be made.

Damage in the form of transverse cracking in cross-ply graphite/epoxy laminates has been studied by the use of these two techniques. For through-the-thickness measurements the stiffness was found to be insensitive to transverse cracking. The attenuation, however, was found to be quite sensitive and, therefore, has been shown to be a reliable

## 20. DISTRIBUTION/AVAILABILITY OF ABSTRACT

UNCLASSIFIED/UNLIMITED

SAME AS RPT

 DTIC USERS

## 21. ABSTRACT SECURITY CLASSIFICATION

Unclassified

## 22a. NAME OF RESPONSIBLE INDIVIDUAL

Major G. Haritos

22b. TELEPHONE NUMBER  
*(Include Area Code)*

(202) 767-0463

## 22c. OFFICE SYMBOL

## ABSTRACT

It is well-known that composite materials develop a complex damage state when they are subjected to monotonic or fatigue loading. The damage has, in general, two effects on the propagation of an ultrasonic wave: it decreases the stiffness and increases the attenuation. The central objective of this work has been to correlate damage states with changes in the two ultrasonic parameters (wavespeed and attenuation).

We have developed a new technique for measuring the wavespeed and attenuation in the thickness direction, in extremely thin laminates. We have also developed a technique for the excitation and detection of Lamb waves in the lengthwise direction. Thus both the in-plane and out-of-plane measurements can be made.

Damage in the form of transverse cracking in cross-ply, laminates has been studied by the use of these two techniques. For through-the-thickness measurements the stiffness was found to be insensitive to transverse cracking. The attenuation, however, was found to be quite sensitive and, therefore, has been shown to be a reliable damage metric. For the complementary case of Lamb wave propagation in the lengthwise direction, both the stiffness and the attenuation were observed to be sensitive damage parameters.

Accession For	
NTIS GRAAL	<input checked="" type="checkbox"/>
REF ID:	<input type="checkbox"/>
UNCLASSIFIED	<input type="checkbox"/>
DATA ELEMENTS	<input type="checkbox"/>
Distribution	
Availability Codes	
SAC/Region/	
Dist	Serial
A-1	

## 1. SUMMARY OF RESEARCH ACCOMPLISHED

The following is a brief summary of the research performed during the grant period:

- 1.1 A theoretical investigation of plane wave propagation in a general unbounded anisotropic solid.
- 1.2 A combined theoretical/experimental study of plane wave propagation, in the thickness direction, in a composite plate immersed in water.
- 1.3 A combined theoretical/experimental study of Lamb wave propagation, in the lengthwise direction, in a composite plate immersed in water.
- 1.4 A study of damage in the form of transverse cracking by the use of these two techniques

## 2. DETAILS OF RESEARCH ACCOMPLISHED

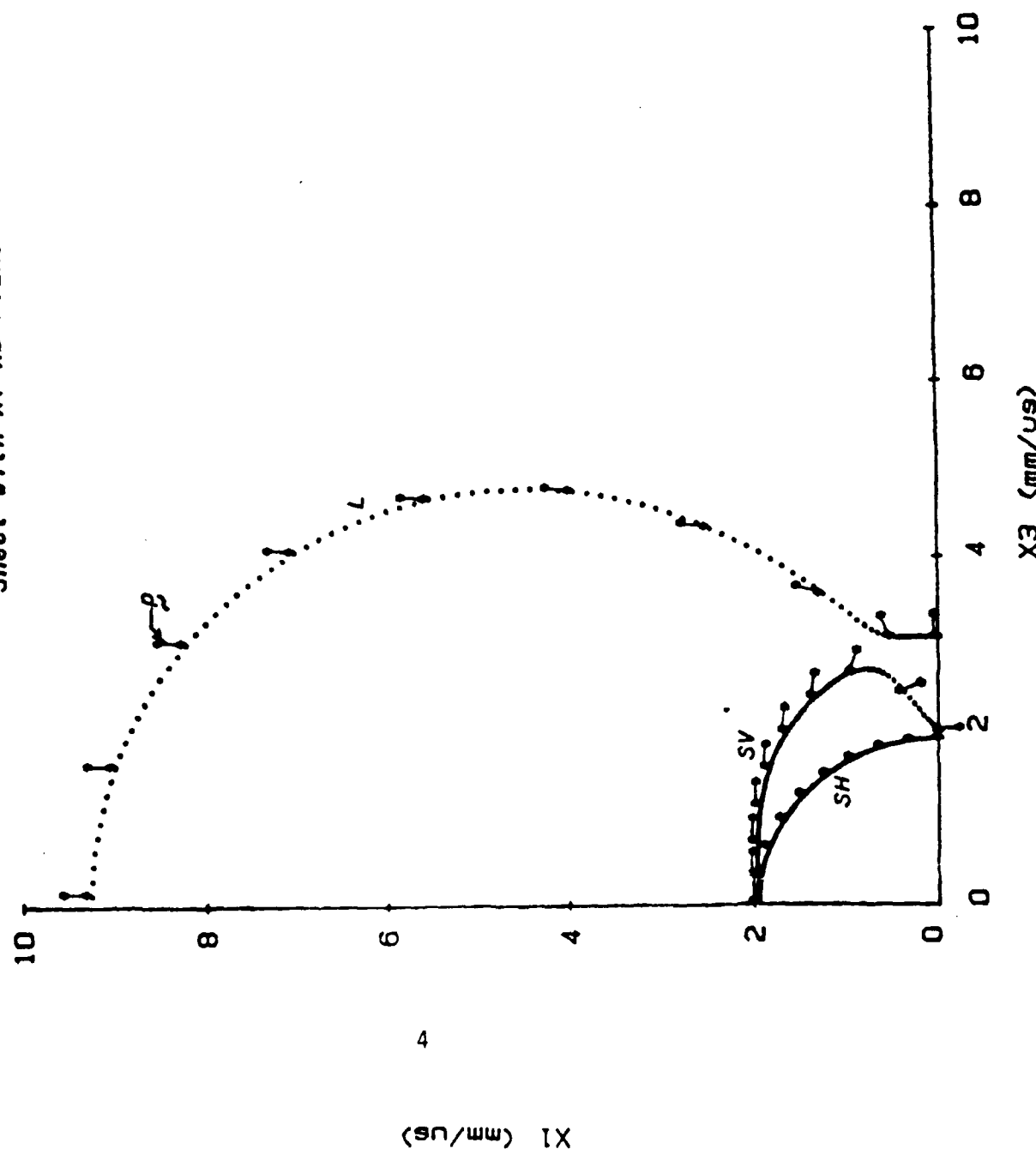
### 2.1 Wave Propagation in an Anisotropic Solid

As a prelude to the design of experimental techniques and the interpretation of the gathered data it was considered desirable to study, in fairly general terms, the nature of wave propagation in anisotropic media. In particular, several wave propagation concepts which are unique to anisotropic media were studied in detail: velocity surface, wave surface, slowness surface, group velocity, and deviations of the energy flux vector and particle displacement vector from the wave vector. These results were summarized in an interim progress report to the AFOSR [1]. In the following we reproduce a typical result of [1]. A generic unidirectional fiber-reinforced graphite/epoxy composite is considered; the fibers are along the  $x_1$  axis (transverse isotropy with  $x_1$  as the axis of isotropy). Fig 1 shows the velocity surface i.e. the distance between the origin and any point on the curve is the velocity of a plane wave in that particular direction. The velocity is an eigenvalue of the well-known Christoffel equations

$$(C_{ijk\ell} n_j n_\ell - \rho v^2 \delta_{ik}) p_k = 0 \quad (1)$$

where  $C_{ijk\ell}$  is the stiffness matrix,  $\rho$  is the density,  $p_k$  is the unit particle displacement vector (eigenvector) and  $v$  is the phase velocity of time-harmonic waves travelling in the direction  $n_i$ . Eq (1) has three eigenvalues: one quasi-longitudinal (L) and two quasi-shear (SH and SV) . Note that, as expected, the highest wavespeed is that of the longitudinal wave in the fiber direction. The unit vector  $p$  is the particle displacement vector. This brings out clearly a unique feature of wave propagation in anisotropic materials: particle displacement in general is not parallel (perpendicular) to

0 DEG. GRAPHITE/EPOXY  
Figure 1: Intersection of Velocity  
Sheet with  $X_1$ - $X_3$  Plane



the wavevector for longitudinal (transverse) waves. In turn, this gives rise to another interesting phenomenon, namely, the direction in which the energy flows is not in the same as the direction of wave propagation. This is shown in Fig. 2. Let slowness  $s = 1/v$ . The slowness surfaces for the longitudinal wave and two shear waves are shown in Fig. 2. It is well-known that the energy flux vector ( $\underline{F}$ ) is perpendicular to the slowness surface; we have plotted  $\underline{F}$  as a bi-directional vector every ten degrees on the slowness surfaces. With reference to the L-surface we note that when the wave is propagating anywhere in the range  $0^\circ - 80^\circ$  from the fiber direction the energy flows (practically) in the fiber direction. This was perhaps the most significant observation of our theoretical investigation.

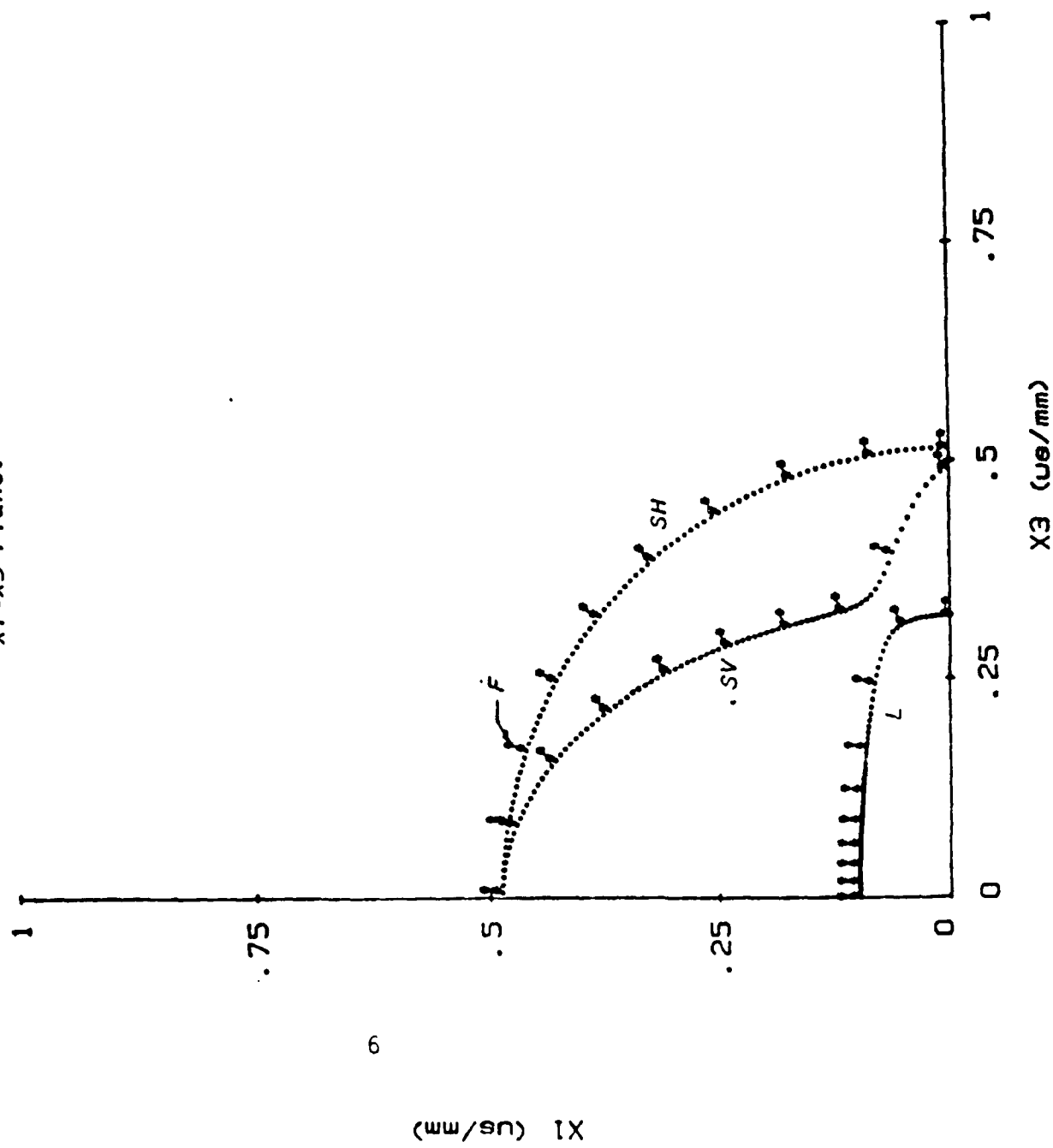
We have developed a computer code which can compute various three-dimensional surfaces for the most general (21 elastic constants) composite material.

The concept of stress-wave-factor originated by Alex Vary [2] has recently been applied to composite materials [3]. To the best of our knowledge there has not appeared a satisfactory explanation as to why the SWF technique works. Our work has offered some (albeit far from complete) explanation of this phenomenon [1].

## 2.2 Through-The-Thickness Measurements. Theory

Our objective here is to measure the wavespeed  $c$  and the attenuation  $k_2$  of a laminate in its thickness direction. A conventional method is the toneburst method [4]. However the toneburst method is suitable only for relatively thick specimens (about five-wavelength thick). The central objective of the development of composite materials is to fabricate light-weight aerospace structures i.e. to use thin laminates (of the order of a few

**SLOWNESS SURFACES- 0 DEG. GRAPHITE/EPOXY**  
*Figure 2: Slowness Sheet Intersection with  
X1-X3 Plane.*



millimeters); here the toneburst method completely breaks down. This observation motivated us to define the first goal of the present research: to develop a new experimental technique suitable for thin plates (sub-millimeter in thickness).

We have used the following fact from the theory of Fourier Transforms: If two events are very close in the time domain, then a pair of corresponding events are proportionately far apart in the frequency domain.

In order to make our technique useful in other areas of mechanics and physics of solids, throughout this investigation we have adapted a "black-box" approach i.e. one can measure the phase velocity, the group velocity and the attenuation of any linear viscoelastic solid. The technique works equally well for thick or thin plates, for dispersive or non-dispersive materials. The details of this technique have been given in [5]. Consider a linear viscoelastic plate (e.g. a composite laminate) immersed in an elastic fluid (e.g. water). A plane-fronted longitudinal wave begins to travel at time  $t=0$  in the positive  $x$  direction; see Fig. 3 for a Lagrangian diagram. Let the displacement in the incident field, Ray 1, be given by

$$u^{\text{inc}} = f_0(\omega t - k_0 x)$$

where  $\omega$  is the circular frequency and  $k_0$  is the wavenumber in water; the speed of sound in water  $c_0 = \omega/k_0$ . The interaction of this pulse with the plate results in a series of reflected pulses, Rays 2, 6, 10, ..., and a series of transmitted pulses, Rays 4, 8, 12, ..., see Ref [5] for details.

We recall the Fourier transforms of a function  $f(t)$  as

$$F^*(\omega) = (2\pi)^{-\frac{1}{2}} \int_{-\infty}^{\infty} f(t) e^{-i\omega t} dt, \quad -\infty < \omega < \infty$$

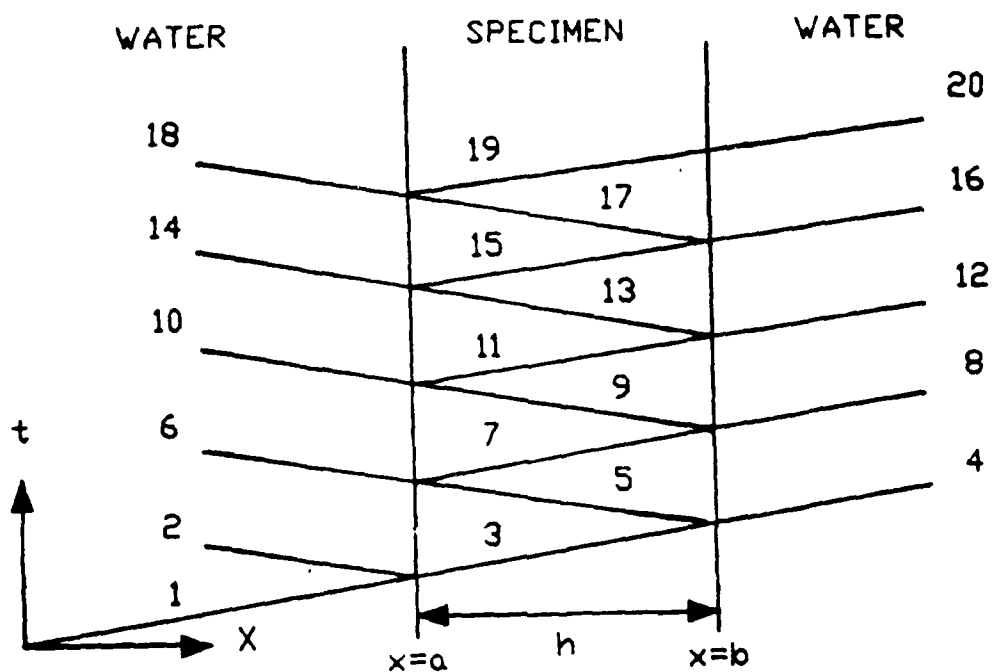


Fig. 3 Lagrangian diagram for reflected and transmitted field from a plate immersed in water.

$$\text{with } f(t) = (2\pi)^{-\frac{1}{2}} \int_{-\infty}^{\infty} F^*(\omega) e^{ti\omega t} d\omega, \quad -\infty < t < \infty$$

### 2.2.1 Thick Specimens

The use of the words "thick" and "thin" is, of course, quite arbitrary. For the purpose of this discussion we define a specimen to be thick if, in Fig. 3, we can clearly separate various pulses from each other. The incident wave is the signal produced by a typical ultrasonic transducer when energized by a short-duration electrical spike.

Let us first consider the reflected field. Let  $f(t)$  be the signal corresponding to Ray 2 and  $g(t)$  be the signal corresponding to Rays 2 and 6 combined; let  $F^*(\omega)$ ,  $G^*(\omega)$  be their Fourier transforms, then [5]

$$\frac{G^*(\omega)}{F^*(\omega)} = 1 - T_{12}T_{21}e^{-12kh}$$

where  $T_{12}$  is the transmission coefficient from water into specimen,  $T_{21}$  is the transmission coefficient from specimen into water,  $h$  is the specimen thickness and  $k$  is the complex-valued wavenumber in the specimen,  $k = k_1 + i k_2$ , where the phase velocity  $c = \omega/k_1$  and  $k_2$  is the attenuation (nepers/mm) i.e. a wave decays exponentially as  $e^{-k_2 x}$ . The stiffness, in turn, is given by an expression of the type  $E = \rho c^2$ . Thus, the measurement of  $k$  is the central objective of this work. If one writes  $-(G^*/F^*)/T_{12}T_{21}$  in its polar form as  $Me^{i\phi}$ , then it can be readily shown that

$$k_1 = -\phi/2h$$

$$k_2 = (\ln \gamma)/2h$$

Furthermore, a plot of  $|G^*(\omega)|$  vs  $\omega$  is characterized by a series of resonance peaks whose spacing is given by

$$\Delta\omega = (c\pi)/h$$

As was mentioned earlier this is a fundamental observation of this work. As the plate becomes very thin ( $h \rightarrow 0$ ) the front and back surface reflections become very close in the time domain; however,  $\Delta\omega \rightarrow \infty$  i.e. any two neighboring resonance peaks in the frequency domain (the corresponding pair of events) become very far apart.

Let us now consider the transmitted field for a thick specimen. Let  $f(t)$  be the incident field with the specimen removed. Let  $g(t)$  be the signal due to Ray 4 alone. Then

$$\frac{G^*}{F} = T_{12} T_{21} e^{-i(kh + k_0 h)}$$

### 2.2.2 Thin Specimens

Consider a case when  $h$  is so small that Rays 2, 6, 10 ... cannot be separated in the time domain. As previously mentioned, none of the existing techniques can be used to measure the phase velocity or attenuation for this case.

Let  $g(t)$  be the total reflected field, Rays 2+6+10+ ... . Let  $f(t)$  be Ray 2 obtained separately (see [5] for details). Then the complex wavenumber  $k$  can be obtained from the set of equations

$$R_{21}^2 e^{-i2kh} = z,$$

$$z = \epsilon (1+\beta),$$

$$\beta = \frac{R_{12}R_{21}}{T_{12}T_{21}} \left( \frac{G^*}{F^*} - 1 \right)$$

We now consider the transmitted field. Let  $f(t)$  be the incident field through water only i.e. with the specimen removed. Let  $g(t)$  be the total transmitted field, Rays 4+8+12+... . Unlike the cases considered so far, here we get a quadratic in  $Z = \exp(-i\hbar k)$

$$Z^2 + ZY - D_0 = 0, \text{ where}$$

$$Y = \frac{T_{12}T_{21}}{R_{21}Z_0} \frac{F^*}{G^*}$$

$$Z_0 = \exp(-i\hbar k_0)$$

$$D_0 = 1/R_{21}^2$$

The fact that one gets two roots for the wavenumber is not at all disturbing. For the correct root the phase of  $z$  decreases with frequency (for the incorrect root the converse is true)

This sums up the development of the theory in support of the experimental work which is described next.

### 2.3 Through-the-Thickness Measurement. Experimental

A schematic of the apparatus is shown in Fig. 4. The heart of the system is a pair of accurately matched, broad-band, water-immersion piezoelectric transducers. The frequency was varied in the range 0.5 - 10 MHz; the oscilloscope digitizes at the rate of  $100 \times 10^6$  points per second. We estimated the precision of our experiments as follows: For homogeneous materials (e.g. aluminum, epoxy, steel, plexiglas, etc.) the precision in velocity is about 0.1%. For graphite/epoxy composite the precision in velocity is 0.2% and in attenuation it is about 5%.

Calibration Procedures Whenever a new technique for measuring wavespeed (or attenuation) is developed, properly it should be used to measure wavespeed of a material whose wavespeed is known to an accuracy about ten times better than the (claimed) accuracy of the new experimental technique. Unfortunately, however, we found that the National Bureau of Standards has not yet developed a reference standard for wavespeed (or stiffness). This section is devoted to our efforts in lieu of a standard calibration.

### ASTM Round Robin Test

Our laboratory participated in a six-laboratory round-robin program conducted by the American Society for Testing and Materials. Two nickel-based alloys were tested. We measured both the longitudinal as well as the shear wavespeeds. We make two observations.

1. The precision in our measurements was  $\pm 0.15\%$
2. Measurements by all six laboratories were within  $\pm 2.5\%$  of each other

The results of this investigation have been accepted for publication by the Journal of Testing and Evaluation [6].

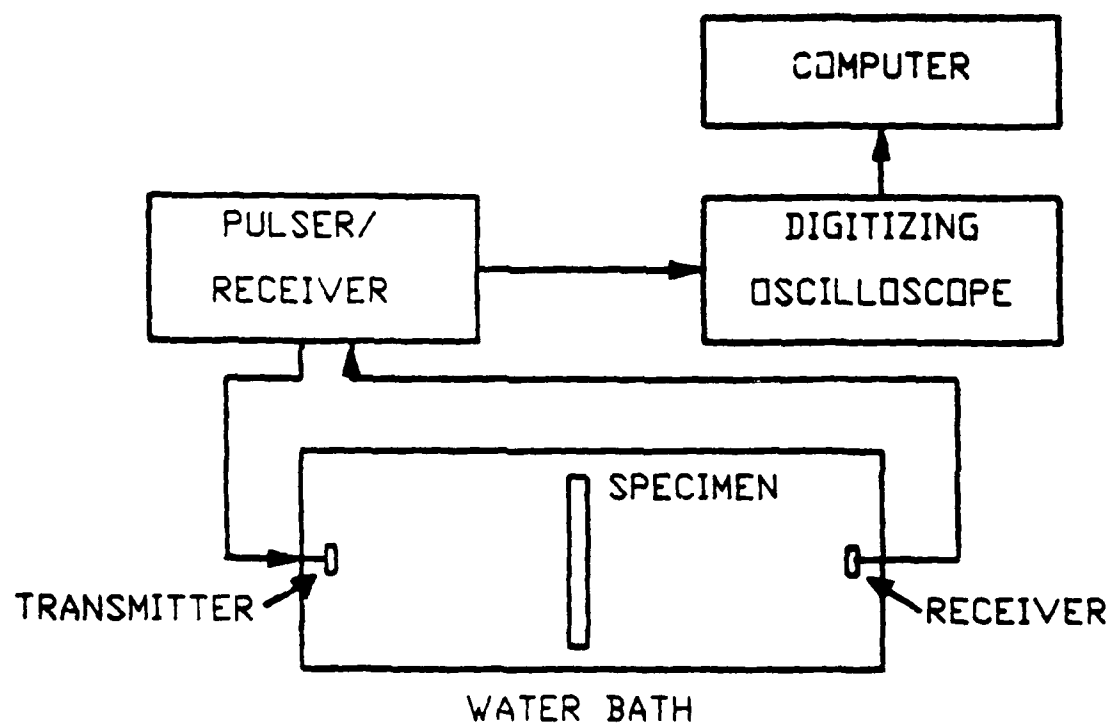


Fig. 4 Block diagram of the apparatus.

Since the goal of our effort is to develop a technique for testing "thin" plates, we subjected our procedures to the following critical test. We started with a "thick" aluminum plate (2.807 mm) and gradually machined it down to an extremely "thin" plate of 0.258 mm thickness ( $10 \times 10^{-3}$  inches i.e. a very thin foil). At each stage we measured the wavespeed. The results are presented in Table 1. (Here,  $\bar{\sigma}$  is the standard deviation of ten measurements for each thickness). We conclude that as we transition from "thick" to "thin" plates, the precision remains within  $\pm 0.15\%$  which is considered excellent. Similar results were obtained with an epoxy specimen [5].

Finally, we subjected our technique to a very difficult test of measuring wavespeed and attenuation in a highly dispersive as well as attenuative medium namely, a random particulate composite. This material has been studied in detail by Kinra et al [7,8], therefore, we had a database with which we could compare our present measurements. The results are shown in Fig. 5. Here  $\langle c_1 \rangle$  is the wavespeed in the composite,  $c_1$  is the wavespeed in the neat matrix material,  $\omega$  is a suitably normalized frequency and  $\tilde{c}$  is the volume fraction of inclusions. The important point is that the entire dispersion curve ( $\langle c_1 \rangle$  vs  $\omega$ ) as well as the attenuation curve was obtained in a single experiment. Previously, ([7,8] for example) each data point required a separate toneburst experiment. Therefore, the new technique is not only more time-efficient by several orders of magnitude, it is also more accurate by about one order of magnitude.

TABLE 1. Test Results on Aluminum Sample

Material: Aluminum  
Wave Type: Longitudinal  
Mode: Transmission  
Frequency: 10 MHz  
Density:  $2.8177 \pm 0.0004$  g/ml

$h$ mm	$h/\lambda$	c mm/ $\mu$ sec	$\bar{\sigma}/c$ %	Technique
2.807	4.4	6.3572		Toneburst
2.807	4.4	6.3239	0.013	Second/First
2.807	4.4	6.3275	0.010	A11/First
1.686	2.7	6.3461	0.040	A11/First
1.001	1.6	6.3538	0.030	A11/First
0.613	0.96	6.3594	0.130	A11/First
0.258	0.4	6.3231	0.140	A11/First

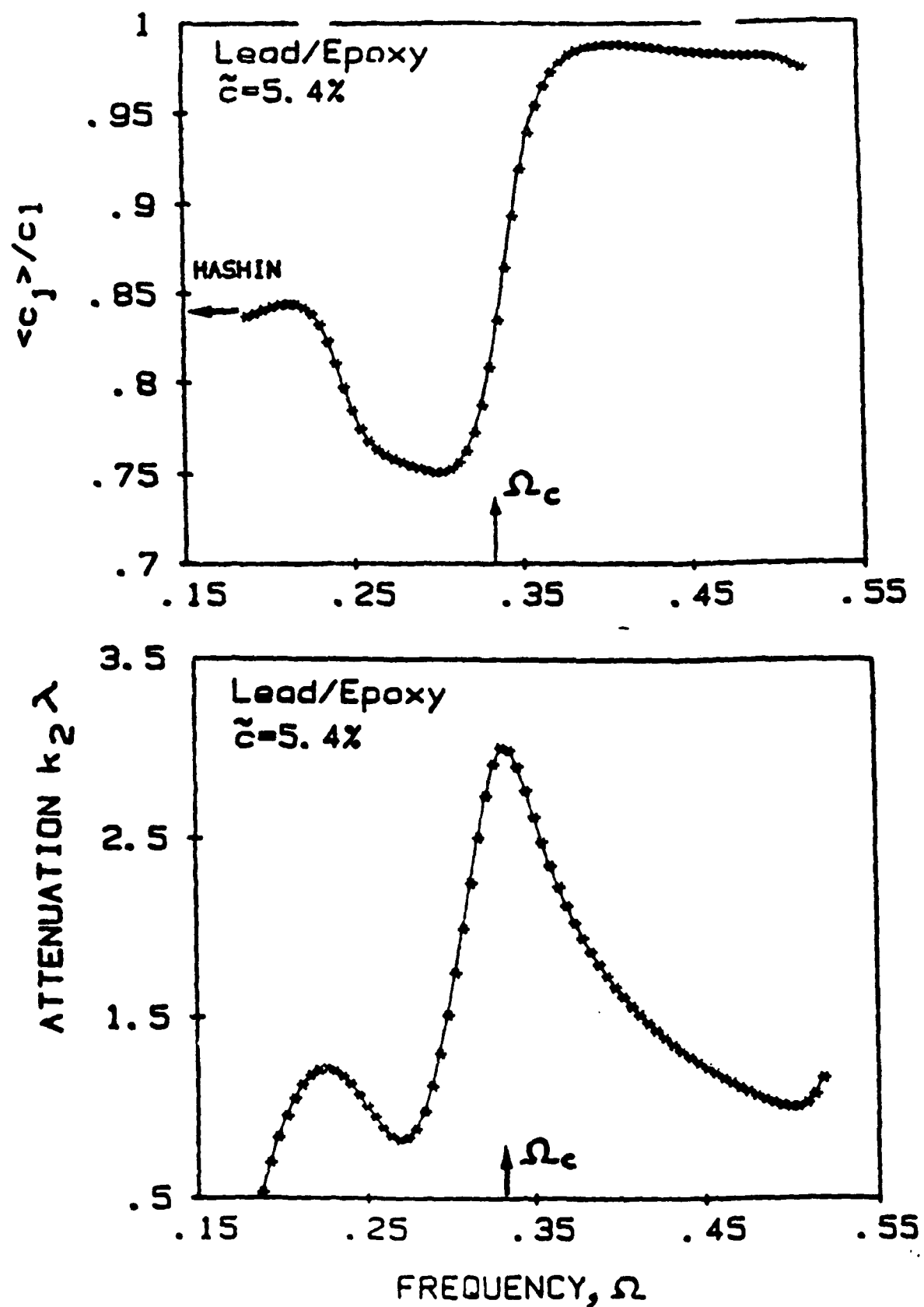


Fig. 5 Velocity and attenuation versus frequency for a highly dispersive medium.

## 2.4 Through-the-Thickness Measurements. Results

We now present some results concerning the assessment of damage using the techniques developed during this investigation. The attention thus far has been confined to cross-ply laminates. Both the "thick" and the "thin" laminates have been tested. The principal conclusions are:

1. As expected, there is no measurable change in the through-the-thickness stiffness due to transverse cracking
2. The attenuation, on the other hand, is a very sensitive and reliable measure of transverse cracks.

Following lay-ups were tested:  $[0_2, 90_8, 0_2]_S$ ,  $[0_6, 90_4, 0_2]_S$ , and  $[0, 90_4]_S$ . The laminates were subjected to monotonic tensile loading and transverse cracks developed in the  $90^\circ$  plies. The "damage" was quantified in the form of edge replication; see Fig. 6. After each of the six load steps, the coupon was removed from the tensile testing machine and subjected to an ultrasonic examination. In Fig. 6 we have plotted the change in attenuation from its undamaged state,  $\Delta k_2 \lambda$ , against the load level; the damage state at each load level is included schematically. We have shown only that one inch segment of the length of the coupon which is insonified by the ultrasonic beam. It is well-known that the scattering of a wave by a defect is a sensitive function of the wavenumber,  $k_1 a$ , when  $k_1 a$  is of the order of one, where "a" for a crack is the half-crack length. To study the influence of  $k_1 a$  we conducted tests at three different frequencies, namely, 2.25, 5.0 and 7.5 MHz where  $k_1 a = 1.25, 2.7$  and  $4.0$ , respectively. In Fig. 6 we observe that  $\Delta k_2 \lambda$  increases dramatically with damage, it is therefore a sensitive measure of damage. In particular, we note that in going from damage state 3 to 4, only one additional crack appears. . . the increase in attenuation is quite significant and substantially greater than the error of measurement which is

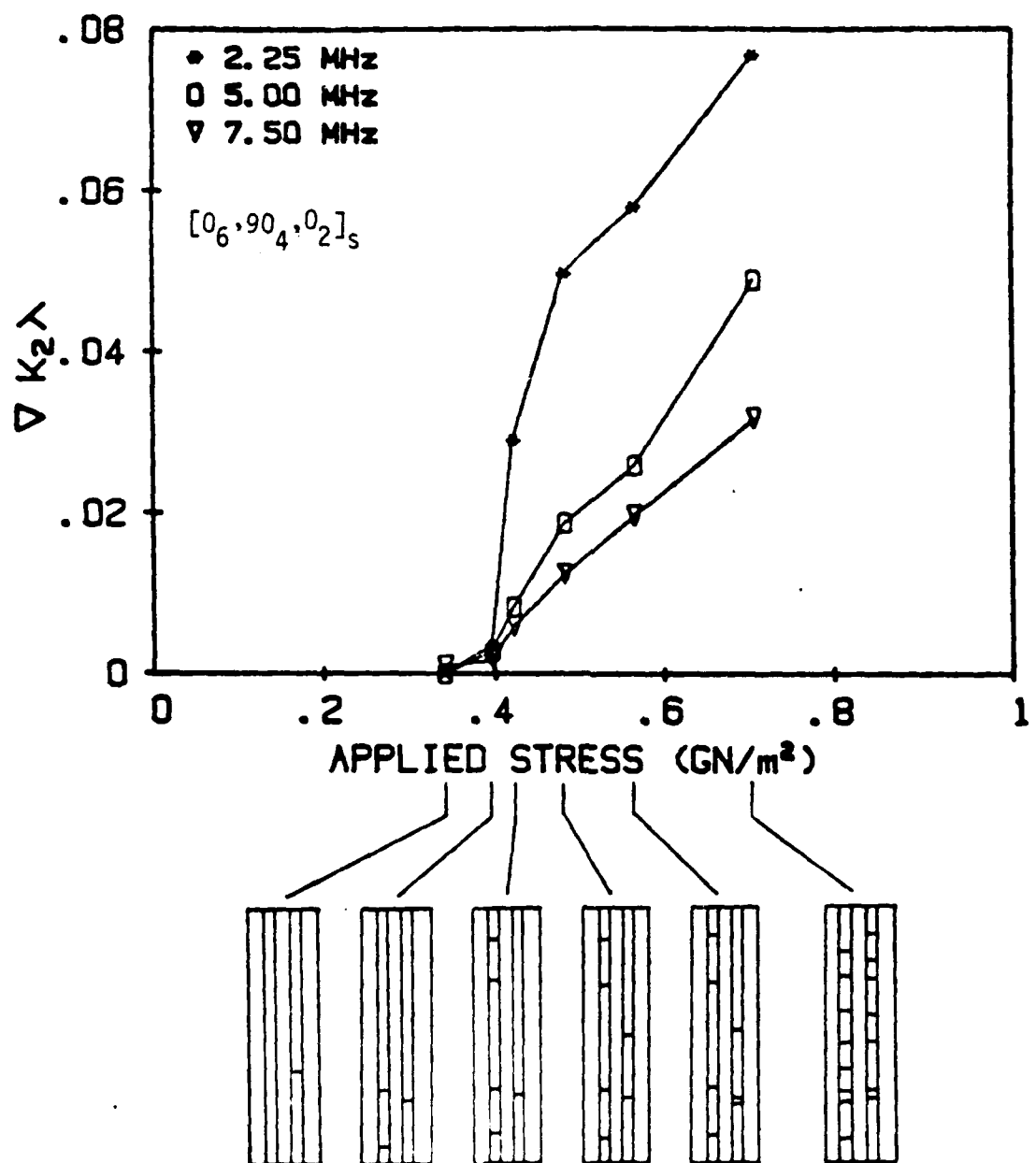


Fig. 6 Attenuation versus damage (transverse cracking) at one location and three frequencies.

estimated to be about  $\pm 5\%$  ( $k_2\lambda$  is of the order of 0.2).

The damage in composite materials is not distributed uniformly; in fact, by now it is fairly well accepted that it is a stochastic phenomenon. In view of this we monitored damage at three different locations along the length of the beam with the following extremely important objective in mind. Damage is a function of the history of loading. Yet our technique should measure only the current state of damage and should be independent of the past history. Therefore, in Fig. 7, we have plotted attenuation versus damage at three different locations and at three different frequencies; here damage is defined as the cumulative crack length i.e. number of transverse cracks times the crack length which, for the present case of  $[0_690_40_2]_s$  is the thickness of the  $90_4$  group of plies i.e. 0.5 mm. Indeed, the three curves coincide within the errors of measurement. Thus the curves in Fig. 7 may be viewed as Master Curves for an inversion of the attenuation data to yield a measure of damage.

The corresponding data for the wavespeed at one position is included in Fig. 8. There is virtually no change in the wavespeed with damage. (this is consistent with a well-known fact in fracture mechanics that a crack causes a minimal reduction in the stiffness of a structure in the direction parallel to the crack faces). Finally, for brevity we include here only the final conclusions of some related investigations. The details may be found in Ref. [9].

1. It has been reported at conferences that by using the Stress Wave Factor approach one can predict the site of the final fracture. By using the attenuation as a damage metric we found the converse to be true i.e. one cannot predict the site of the final fracture. We hasten to add that our observation is consistent with the theoretical work of Riebsnider et al at VPI & SU [10].

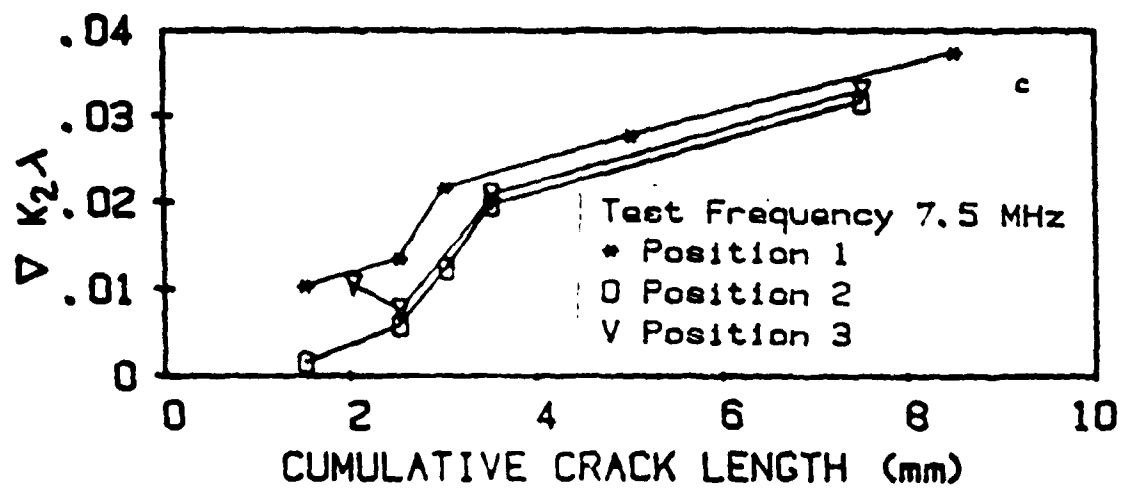
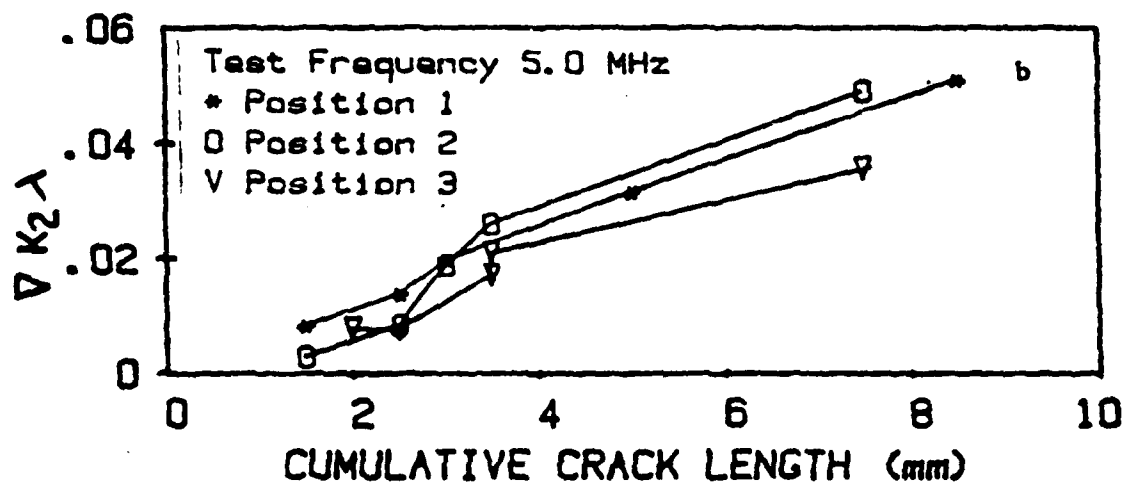
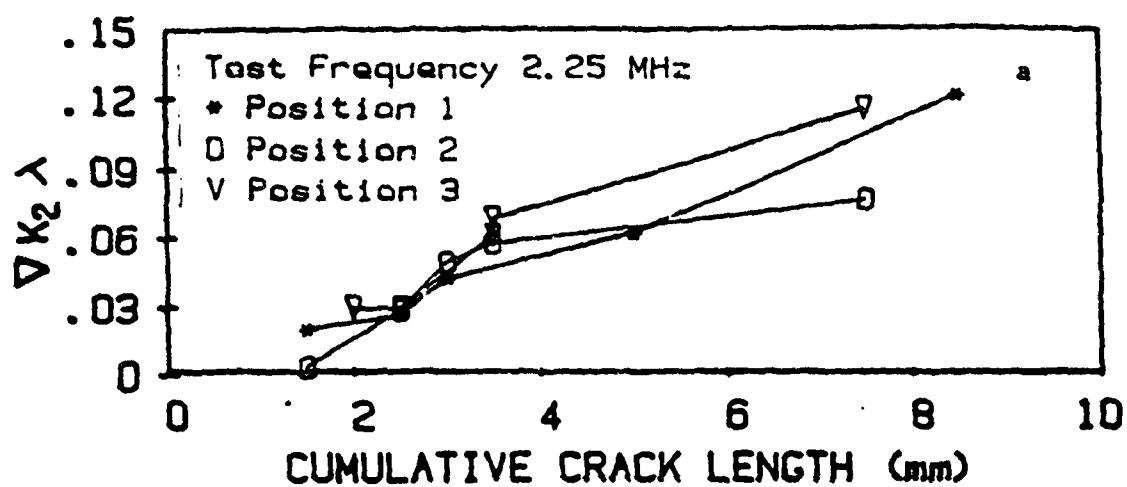


Fig. 7 Attenuation increases with transverse cracking.  
Laminate:  $[0_6, 90_4, 0_2]_S$

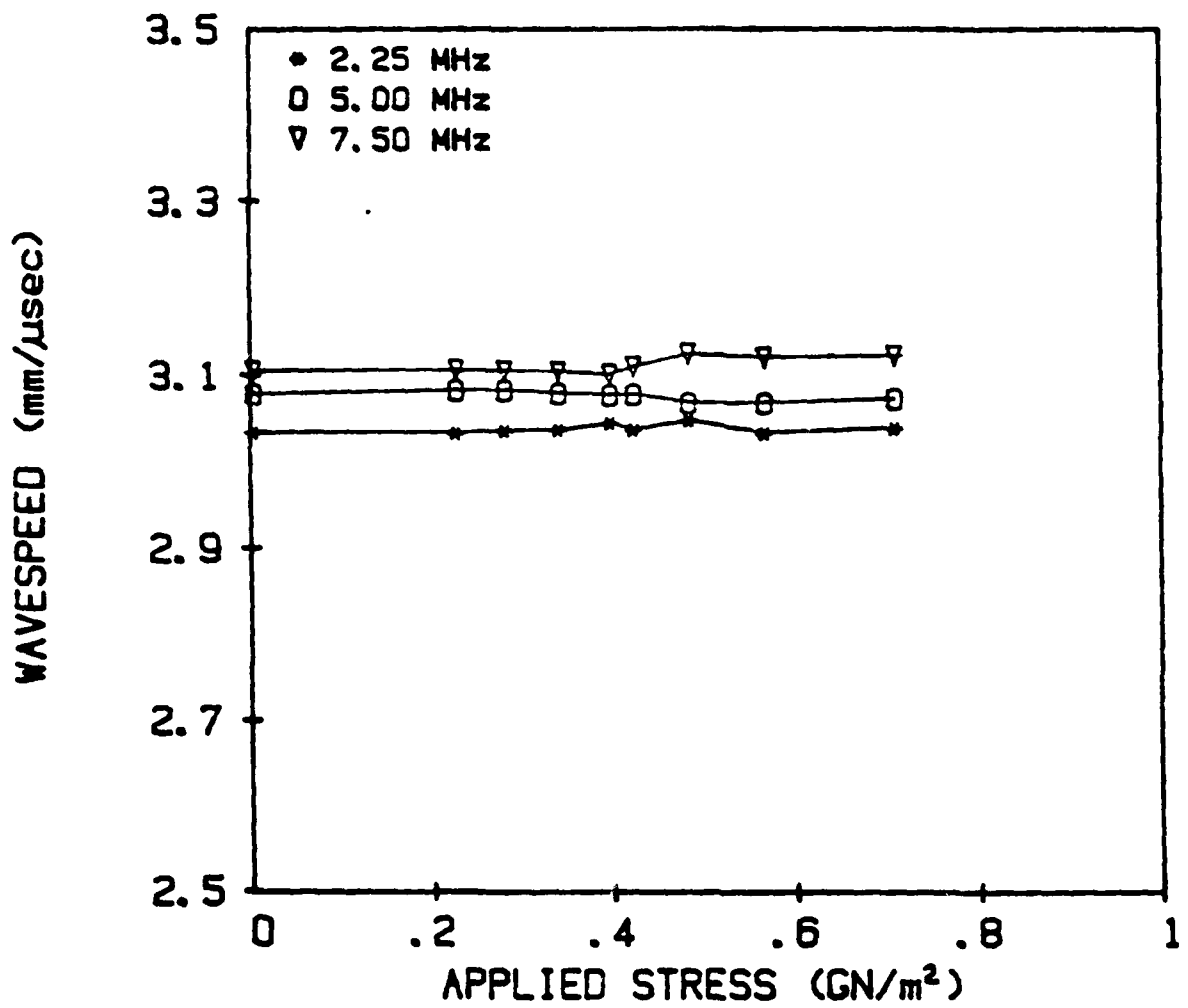


Fig. 8 Wavespeed as a function of applied stress for a  $[0_6, 90_4, 0_2]_s$  laminate.

2. There has been some debate in the literature whether or not the process of unloading, subsequent to the formation of transverse cracks, can cause partial (or even total) crack closure. Our measurements show clearly that some crack closure does take place [9].

### 2.5 Lamb Wave Method. Theory

An extensive literature review concerning the propagation of Lamb waves in an anisotropic plate immersed in a fluid was carried out. Only approximate solutions were found; these have been reviewed in [11]. For the case in hand the density of water is comparable to the density of the composite material. Therefore, the approximate theories - which are based on the assumption that the density of the fluid is small compared to the density of the plate - yield unacceptably erroneous results. This defined the first objective of our work: To obtain an exact analytical solution.

Consider a symmetric composite laminate (not necessarily balanced). Let  $x_1$  and  $x_2$  lie in the plane of the plate; let  $x_3$  be perpendicular to it. The plate occupies the space  $x_3 = \pm b$ . The generalized Hooke's law for such a material is

$$\begin{bmatrix} \sigma_{11} \\ \sigma_{22} \\ \sigma_{33} \\ \sigma_{23} \\ \sigma_{13} \\ \sigma_{12} \end{bmatrix} = \begin{bmatrix} C_{11} & C_{12} & C_{13} & 0 & 0 & C_{16} \\ C_{12} & C_{22} & C_{23} & 0 & 0 & C_{26} \\ C_{13} & C_{23} & C_{33} & 0 & 0 & 0 \\ 0 & 0 & 0 & 2C_{44} & C_{45} & 0 \\ 0 & 0 & 0 & C_{54} & 2C_{55} & 0 \\ C_{61} & C_{62} & 0 & 0 & 0 & 2C_{66} \end{bmatrix} \begin{bmatrix} '11 \\ '22 \\ '33 \\ '13 \\ '13 \\ '12 \end{bmatrix}$$

This relation can be written in the indicial form as

$$\sigma_{ij} = c_{ijkl} \epsilon_{kl} \quad \text{for } i,j,k,l=1,2,3$$

where the strain displacement relation can be written as

$$\epsilon_{ij} = (u_{i,j} + u_{j,i})/2 \quad \text{for } i,j=1,2,3$$

The equation of motion in an elastic medium is

$$\sigma_{ij,j} = \rho \ddot{u}_i$$

The boundary conditions are:

$$\sigma_{31} = 0 \quad \text{and} \quad \sigma_{33} = -p \quad \text{at the plate faces } z = \pm b.$$

Here  $p$  is the pressure at the plate/water interface. The wave motion in water satisfies the equation of motion

$$\frac{\partial^2 \phi}{\partial x^2} + \frac{\partial^2 \phi}{\partial z^2} + k_L^2 \phi = 0$$

The continuity of the normal displacements requires that the displacement in solid ( $u_3$ ) be equal to that in the fluid ( $w_L$ ):

$$u_3 = w_L \quad \text{at} \quad z = \pm b$$

We have solved this boundary value problem for the complex-valued wavenumber  $k_x$  whose real part ( $k_1$ ) is connected to the phase velocity of the

Lamb wave through the relation  $c = \omega/k_1$  and whose imaginary part ( $k_2$ ) is the attenuation of the Lamb wave i.e. the wave decays at  $\exp(-k_2 x)$  in the  $x$  direction. We point out that this is not attenuation in the sense of absorption, for both media are elastic; rather, the wave attenuates because it leaks energy into water as it propagates. It is for this reason that frequently these waves are called "leaky Lamb waves." We now present the final results of our calculation. As with Lamb waves for a plate in air, we get symmetrical (longitudinal) and anti-symmetrical (flexural) waves. The wavenumber  $k_x$  is a root of the transcendental equations.

$$\frac{\tan(k_{zp}b)}{\tan(k_{zm}b)} - \frac{Gp*Hm}{Gm*Hp} + \frac{i\rho_L\omega^2 \tan(k_{zm}b)}{\rho(Gm/\rho) \text{SQR}(k_x^2 - k_L^2)} \left[ -\frac{Hm}{Hp} Rp + Rm \right] = 0.$$

Symmetric Mode

$$\frac{\tan(k_{zm}b)}{\tan(k_{zp}b)} - \frac{Gp*Hm}{Gm*Hp} + \frac{i\rho_L\omega^2 \cot(k_{zp}b)}{\rho(Gm/\rho) \text{SQR}(k_x^2 - k_L^2)} \left[ \frac{Hm}{Hp} - Rp - Rm \right] = 0.$$

Asymmetric Mode

For details of the calculation the reader is referred to [12]. The roots of these equations had to be searched numerically and that was found to be a fairly involved process. Briefly, the modified Newton's (or Secant) method was used in two steps: (1) First, assume  $k$  is real and find the best estimate of  $k$ ; (2) Second, let  $k$  be complex,  $k = k_1 + ik_2$ . Each of the above (complex) equations yields a pair of real equations. A simultaneous numerical solution is then found.

## 2.6 Lamb Wave Method. Experimental

A schematic of the apparatus is shown in Fig. 9. In theory we assumed time harmonic motion; in order to simulate that in a laboratory we use a toneburst i.e. a sinusoidal wave of about 20 cycles duration. All measurements are made away from the two ends of the toneburst (i.e. transients) and near the center of the toneburst. The heart of the system is a pair of accurately matched transducers: one is energized and acts as a transmitter, the other is passive and acts as a receiver. The wave travels as a longitudinal or pressure wave in water. The specimen is inclined to the incident wave at the correct angle for the Lamb wave mode of interest given by the Snell's law:

$$\frac{\sin i}{C_w} = \frac{\sin(\pi/2)}{C_L}$$

where  $i$  is the angle of incidence,  $C_w$  is the speed of sound in water and  $C_L$  is the speed of the particular Lamb wave mode of interest. The leaky Lamb wave in the specimen radiates energy into water symmetrically on both sides; this signal is sensed by the receiving transducer. The attenuation is measured as follows. The receiver is moved gradually in a direction perpendicular to the "line-of-sight" of the transducers. At each step the received amplitude is recorded. An exponential of the type  $\exp(-k_2 x)$  is fitted through the data to obtain  $k_2$ . The velocity is measured as follows. The specimen is rotated gradually and in very fine steps and the correct angle of incidence is that which produces the maximum received amplitude. We stumbled upon an independent (and very elegant) check on the correctness of the angle of incidence. Through a simple calculation [12] we have shown that if one moves the receiver perpendicular to the "line of-sight" then, for the correct angle, the arrival time of a point of constant phase at the receiver remains

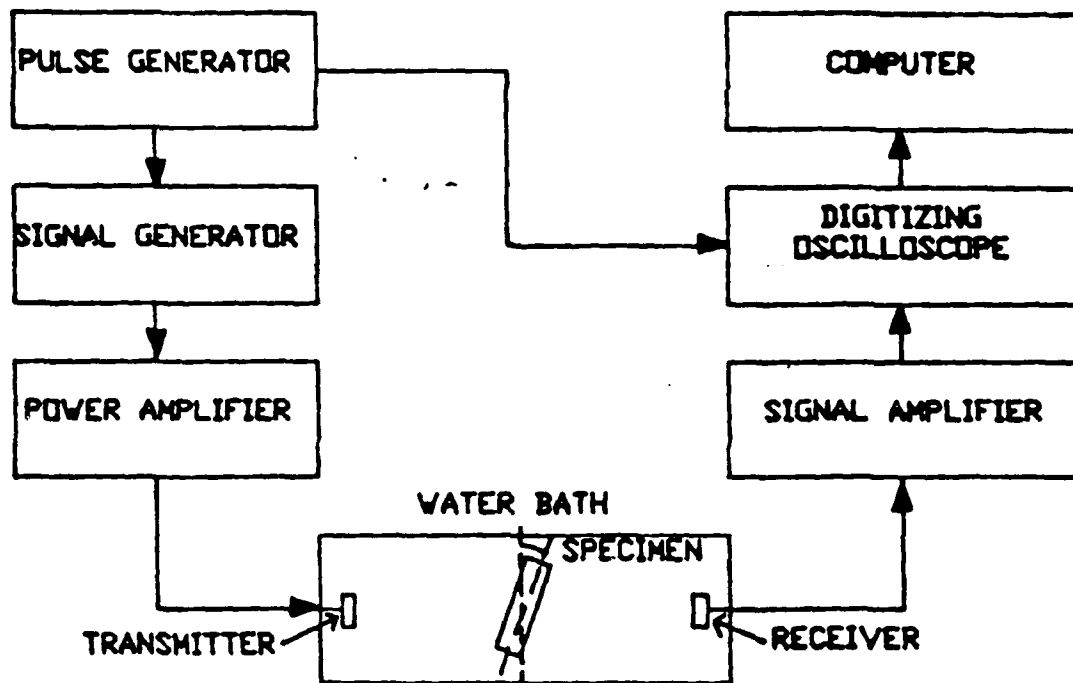


Fig. 9 Block Diagram of the experimental setup.

unchanged; for all other angles the arrival time changes, the magnitude of the change being proportional to the error. Experience indicated this to be a sensitive check on the correctness of the angle of incidence. Having found "i" the speed is calculated from:

$$C_L = C_W / \sin(i)$$

Calibration Procedures The validity of our theory was checked against some earlier calculations as well as against our own experimental results. Our theory was used to calculate the dispersion (wavespeed versus frequency) as well as the attenuation curves for a steel plate in water; the motivation for choosing steel being that Merkulov [13] had earlier reported results for this material. First ten modes of wave propagation were calculated. The agreement with the theory of Merkulov [13] was found to be excellent; see [12] for details.

Next, dispersion and attenuation curves were calculated for an aluminum plate in water; wavespeed and attenuation were also measured; they are compared in Fig. 10. The solid lines are symmetrical (longitudinal) modes, the dashed lines are the anisymmetrical (flexural) modes; the circles are the (discrete) data points; the agreement between theory and experiment is considered remarkably good.

Finally, the dispersion and attenuation curves for an undamaged composite material,  $(0, 90_3)_S$ , are shown in Fig. 11. It was found that it was easier to collect data with the fundamental symmetric mode ( $S_0$ ). The comparison between the theory and the experiment is considered quite satisfactory. In the next section we will apply the Lamb wave method to the assessment of damage.

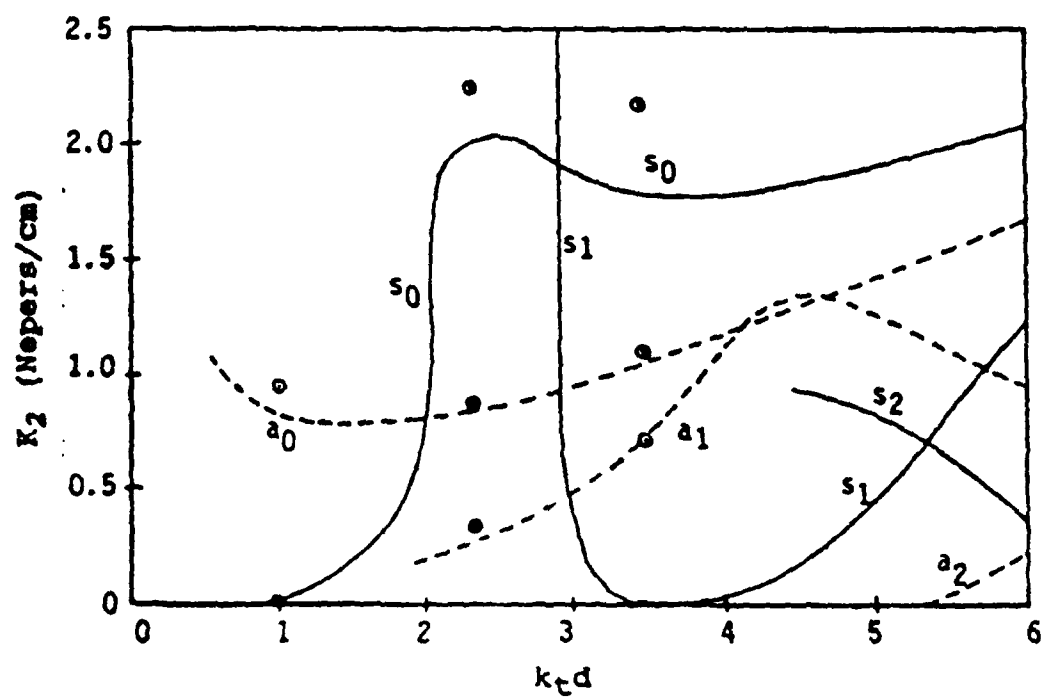
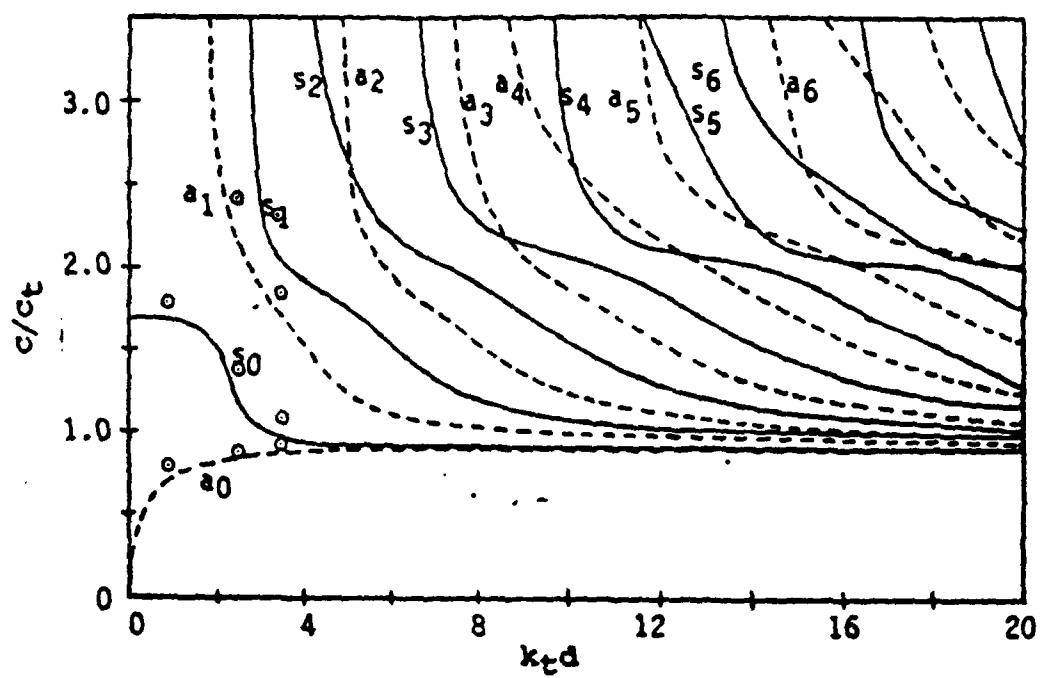


Fig. 10 Dispersion (upper) and attenuation (lower) curves for an aluminum plate in water.

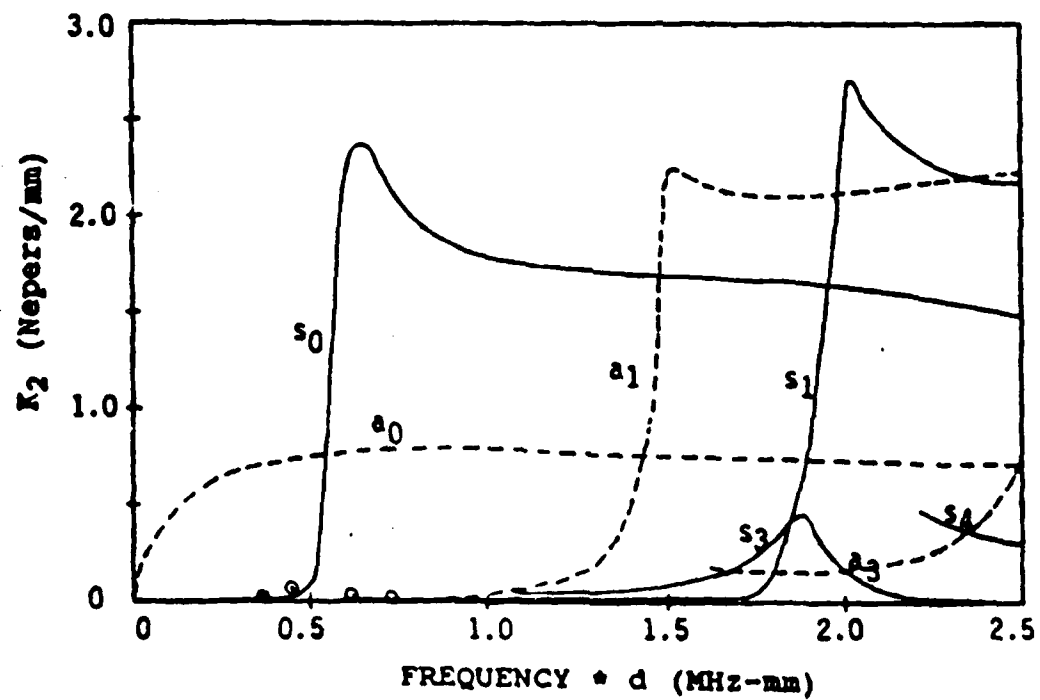
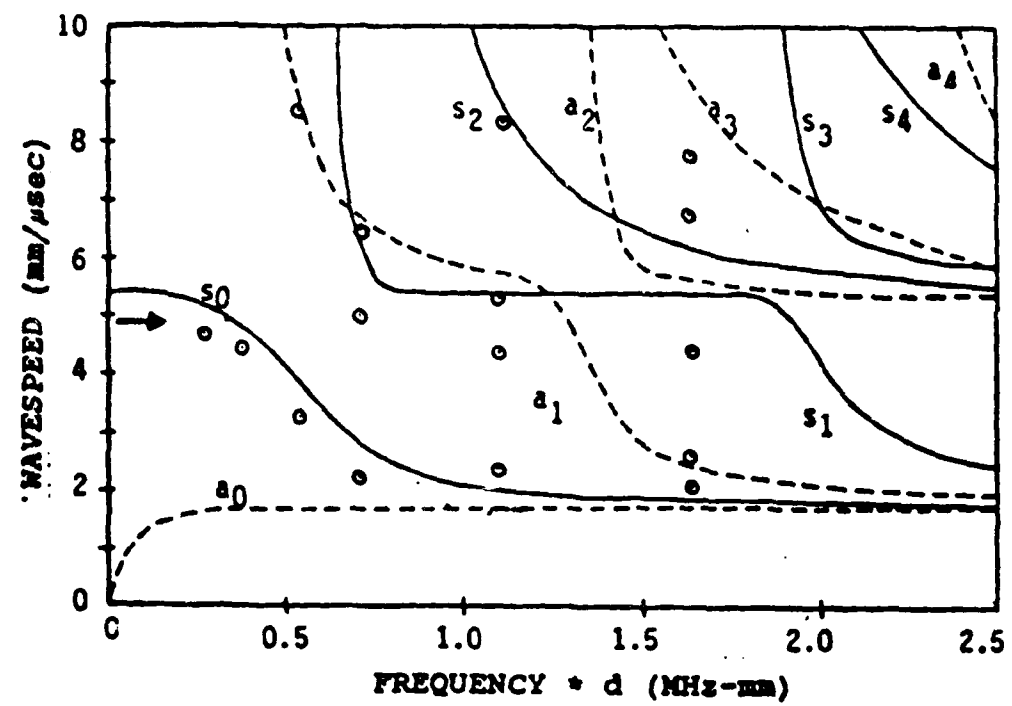


Fig. 11 Dispersion (upper) and attenuation (lower) curves for a  $[0/90]_s$  laminate.

## 2.7 Lamb Wave Method. Results

Three types of laminates were studied:  $[0_2, 90_2 0]_S$ ,  $[0, 90_3]_S$  and  $[0, 90_4]_S$ . The form of damage produced was transverse cracking. As before, the coupons were loaded in an Instron testing machine to various load levels. At each load step the test was interrupted, an edge replication was taken to obtain a record of the transverse cracks and the coupon was subjected to an ultrasonic examination. The loading was then resumed. Several modes of Lamb wave propagation were examined. Experience indicated that the most suitable mode was the fundamental symmetric mode  $S_0$  [14]. All data presented in the sequel were gathered by using this mode. It also turns out that in the long-wavelength limit the dispersion equation for this mode simplifies to

$$c^2 = E_{11}/\rho(1-v_{12}v_{21})$$

and since for the particular lay-ups under consideration

$$v_{12}v_{21} \ll 1,$$

approximately  $c^2 = E_{11}/\rho$

Results concerning  $[0_2, 90_2, 0]_S$  are reported first, see Fig. 12. Note a rather high crack density. The crack occupies the  $90^\circ$ -ply group i.e.  $2a = 0.25$  mm. Because the crack length is so small it is not surprising that the reduction in stiffness is very small, about 5% up to failure. In Fig. 12,  $E_0$

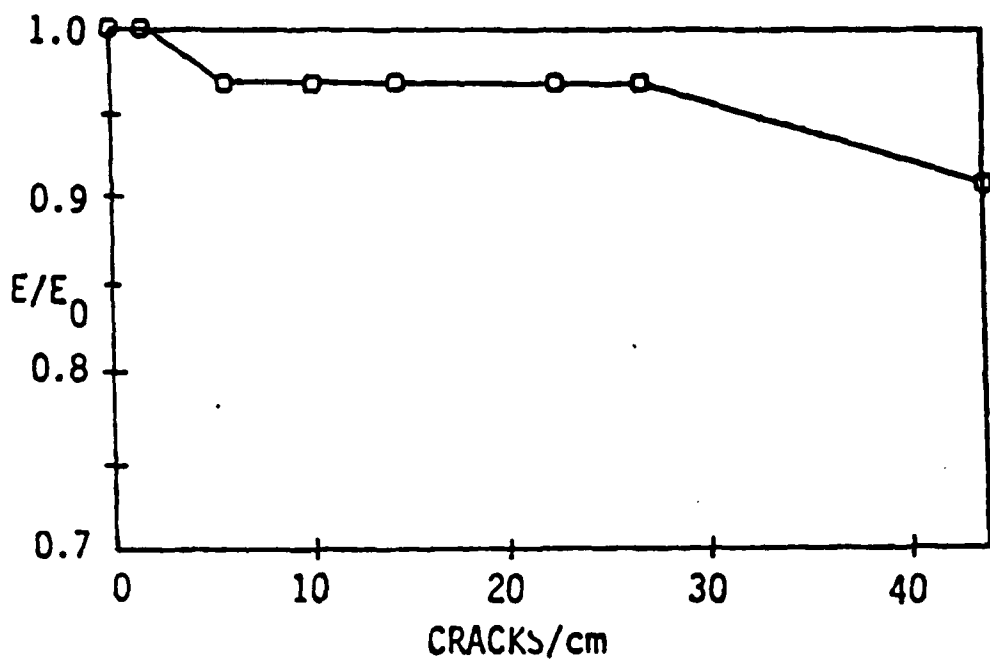


Figure 12 Reduction in stiffness in a  $[0_2 90_2 0]$  laminate,  $f=0.5$  MHz,  $d=0.55$  mm.

is the initial stiffness and  $E$  is the "current" stiffness of the damaged specimen. Next we report results obtained with  $[0,90_3]_S$ , see Fig. 13.; the major difference here is that the  $90^\circ$ -group has six plies i.e.  $2a=0.75$  mm. As a result a relatively greater reduction in stiffness is observed; about 15% to failure. The attenuation measurements are also reported; attenuation is rather small. Next, we consider a  $[0,90_4]_S$  laminate; see Fig. 14. Here the edge replications are also included as is the location of the transmitting transducer (T) and the receiving transducer (R). Note the high density of transverse cracks at the (final) load-step 9. As expected on the basis of the larger crack length, the reduction in stiffness is very large, about 30% to failure.

Of course a crack may be viewed as "small" or "large" depending upon its relation to the wavelength. To this end we have defined a dimensionless wavenumber  $k_1 a = 2\pi f a / C_L$  where  $f$  is the frequency and  $C_L$  is the Lamb wave speed. The data collected with the three different laminates is "unified" into a single plot in Fig. 15. The cumulative crack length is the number of cracks times the crack length,  $2a$ . It is well-known that at the very low wavenumber of  $k_1 a = 0.06$ , we are in the so-called Rayleigh regime of scattering where the cracks act as weak scatters. As a result attenuation is very low. At a slightly higher  $k_1 a = 0.28$ , the attenuation is still rather low. But when  $k_1 a = 0.45$ , we get a substantial attenuation. It is also well-known that at certain critical frequencies cracks begin to resonate (very much like the vibrations of a string) This typically happens when  $k_1 a = 0(1)$ . Figure 15 suggests that we may be approaching resonance. This conjecture is the subject of the current investigation.

In conclusion, we have established that both the wavespeed and the attenuation of Lamb waves serve as measures of damage in composite material.

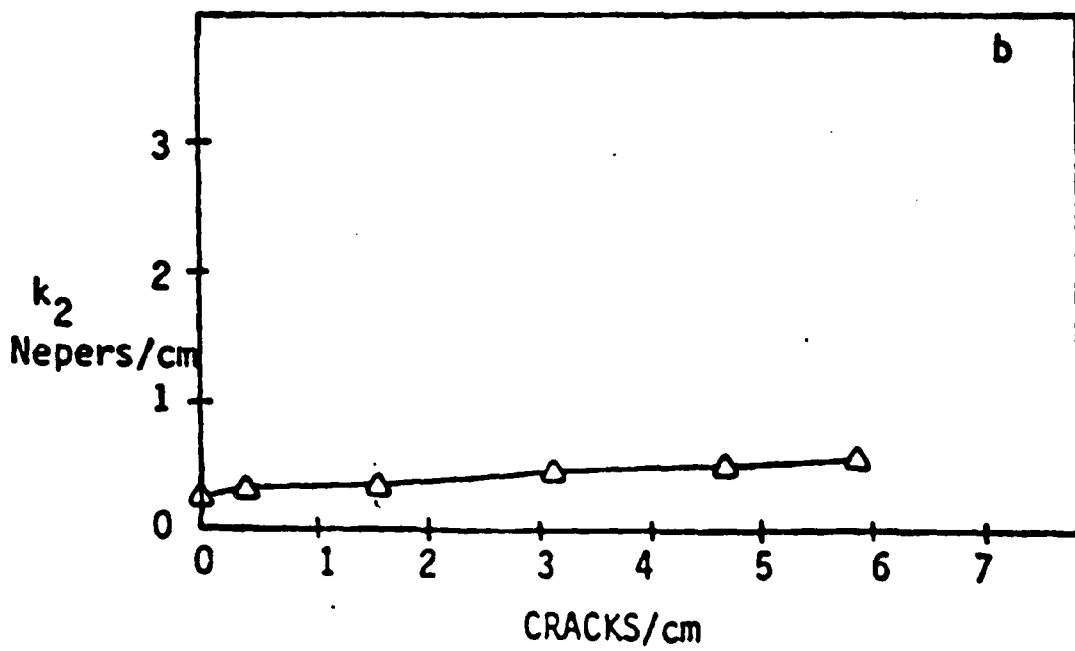
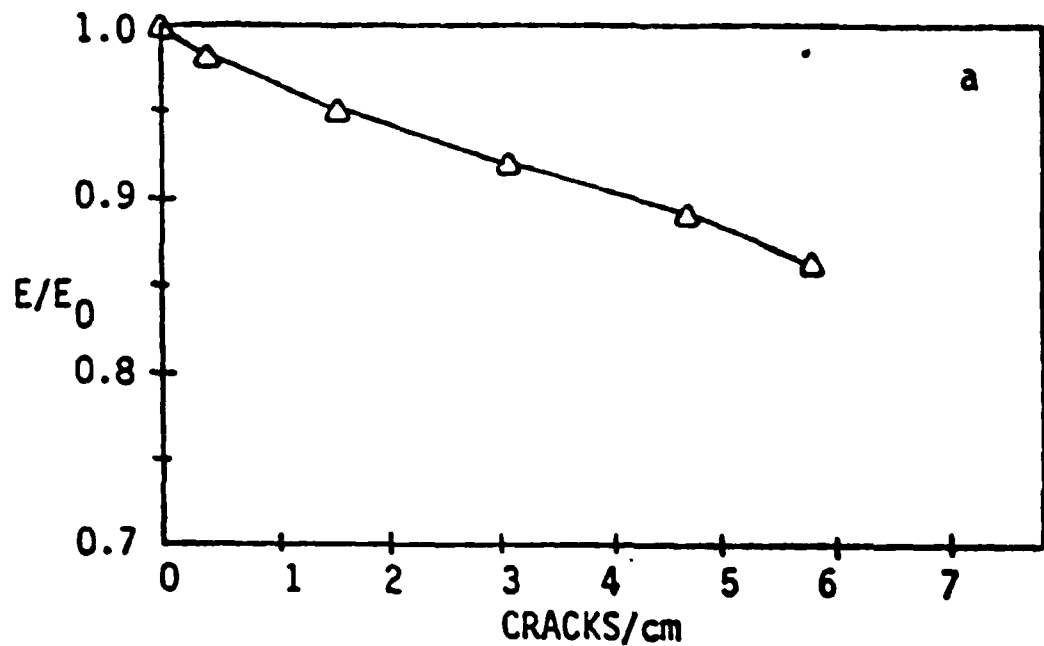


Figure 13 (a) Reduction in stiffness, (b) increase in attenuation in a  $[0 \ 90_3]_s$  laminate,  $f=0.5 \text{ MHz}$ ,  $d=0.55 \text{ mm}$ .

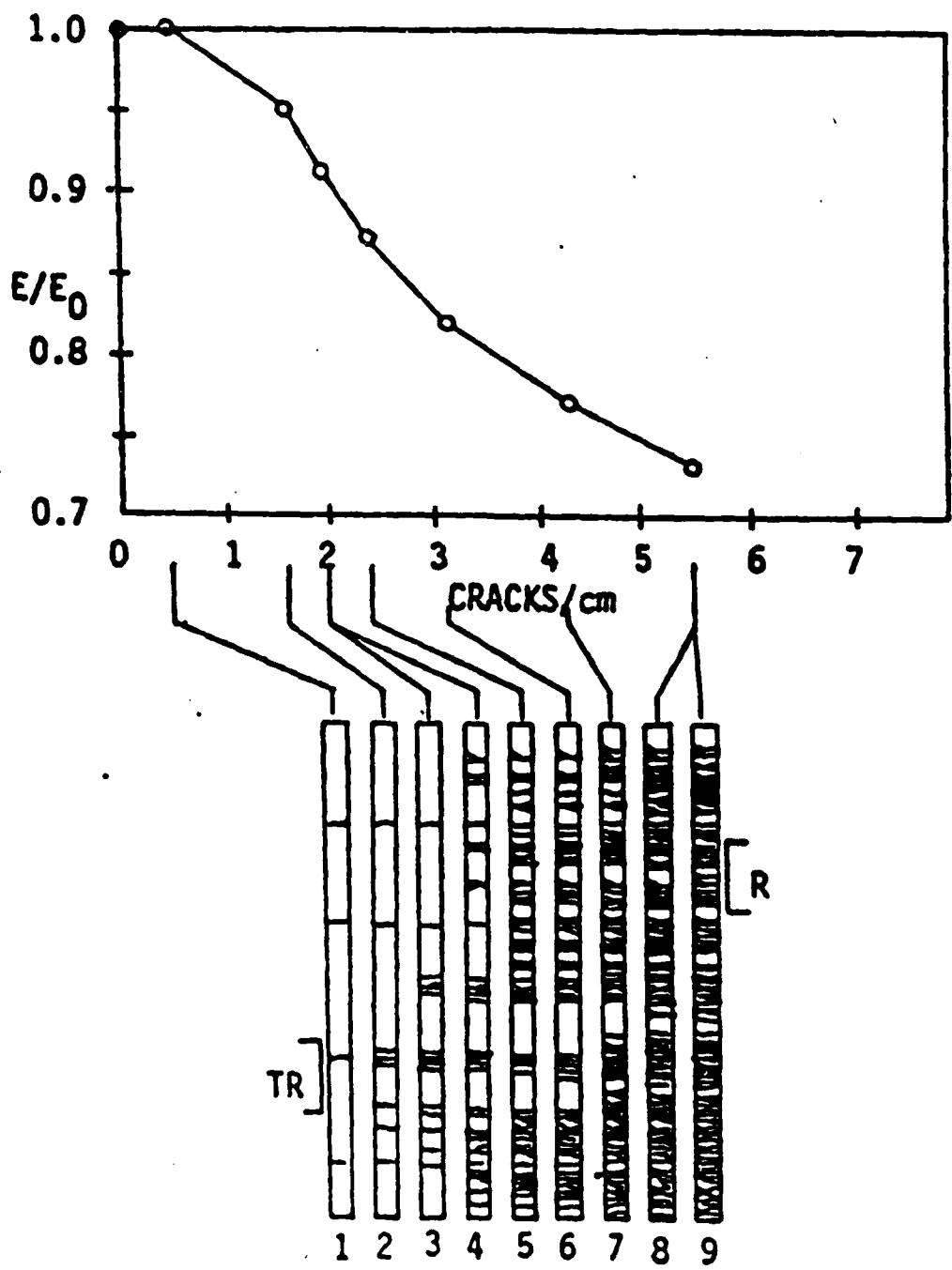


Figure 14 Reduction in stiffness in a  $[0\ 90_4]s$

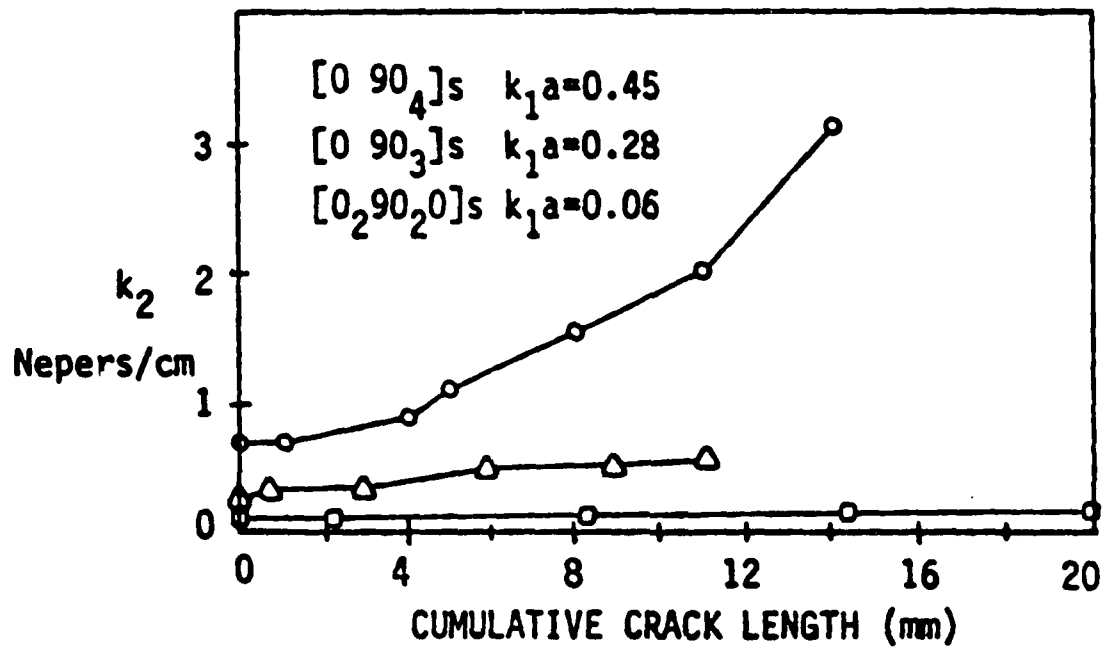


Figure 15 Increase in attenuation ( $k_2$ ) with cumulative crack length for three laminates tested.

## 2.8 References

- [1] J.G. Eden and V.K. Kinra, "Propagation of Elastic Waves in Unidirectional Fiber-Reinforced Composites," Mechanics and Materials Center Report MM 4875-84-19, Texas A&M University (August 1984).
- [2] A. Vary, "Acousto-Ultrasonic Characterization of Fiber-Reinforced Composite Composites," Materials Evaluation, Vol. 40, No. 6, pp. 650-54 (1981).
- [3] E.G. Henneke, J.C. Duke, W.W. Stinchcomb, A. Govada and A. Lemuscon, "A Study of the Stress Wave Factor Technique for the Characterization of Composite Materials," NASA Contractor Report 3670 (February 1983).
- [4] V. K. Kinra, M.S. Petraitis and S.K. Datta, "Ultrasonic Wave Propagation in a Random Particulate Composite," International Journal of Solids and Structures, Vol. 16, pp. 301-312 (1980).
- [5] V.K. Kinra and V. Dayal, "A New Technique for Ultrasonic NDE of Thin Specimens," Experimental Mechanics, (accepted for publication).
- [6] V.K. Kinra, "Dynamics Young's Modulus Measurements in Metallic Materials: Results of Interlaboratory Testing Program," Journal of Testing and Evaluation (authors: Wolfenden, Blessing, Chen, Dayal, Harmouche, Kinra, Liemmens, Phillips, Smith, Tetranova and Wann) (to appear).
- [7] V.K. Kinra, "Dispersive Wave Propagation in Random Particulate Composites," Recent Advances in Composites in the United States and Japan, ASTM STP 864, J.R. Vinson and M. Taya, Eds., American Society for Testing and Materials, Philadelphia, 1985, pp. 309-325.
- [8] V.K. Kinra and C.Q. Rousseau, "Acoustical and Optical Branches of Wave Propagation. Some Additional Results," in Proceedings of an International Symposium on Multiple Scattering of Waves in Random Media and Random Rough Surfaces (Eds.: V.V. Varadan and V.K. Varadan), The Pennsylvania State University, pp. 603-613 (1987).
- [9] V. Dayal, V. Kinra and J.G. Eden, "Non-destructive Testing of Matrix Cracks in Fiber-Reinforced Composites," to be submitted to Experimental Mechanics.
- [10] K.L. Reifsnider, E.G. Henneke, W.W. Stinchcomb and J.C. Duke, "Damage Mechanics and NDE of Composite Laminates," in Mechanics of Composite Materials, Recent Advances, Proceedings of the 1st IUTAM Symposium on Mechanics of Composite Materials held at Blacksburg, VA, August 1982, Z. Hashin and C.T. Herakovich, Eds., Pergamon Press (1983).
- [11] V.K. Kinra and V. Dayal, "Ultrasonic NDE of Fiber-Reinforced Composite Materials - A Review," to appear in the Proceedings of the International Conference on Composite Materials and Structures, Madras, India, January 1988.

- [12] V. Dayal and V.K. Kinra, "Lamb Waves in Anisotropic Plates Immersed in a Fluid. An Exact Solution," to be submitted to Experimental Mechanics.
- [13] L.G. Merkulov, "Damping of Normal Modes in a Plate Immersed in a Liquid," *Soviet Physics-Acoustics*, Vol. 10, No. 2, (1984).
- [14] V. Dayal and V.K. Kinra, "Non-destructive Evaluation of Matrix Cracks in Fiber-Reinforced Composites by Leaky Lamb Waves," Second International Conference on Testing, Evaluation and Quality Control of Composites, Surrey (September 1987).

### 3. LIST OF TECHNICAL PUBLICATIONS

1. V. Dayal, V.K. Kinra and J.G. Eden, "Ultrasonic Nondestructive Testing of Fiber-Reinforced Materials," Proceedings of International Symposium on Composite Materials and Structures, June 10-13, Beijing, China, pp. 899-904 (1986).
2. V. Dayal and V.K. Kinra, "Ultrasonic Nondestructive Testing of Composite Materials," Third U.S.-Japan Conference on Composite-Materials, Tokyo, Japan, 1986.
3. V. Dayal and V.K. Kinra, "Ultrasonic NDE of Composites for Transverse Cracking," Proceedings of the Fall Conference of the Society for Experimental Mechanics, Keystone, Colorado, pp. 17-22 (1986).
4. V. Dayal and V.K. Kinra, "Nondestructive Evaluation of Composite Materials Using Ultrasound,"  
(a) Proceedings of the Society for Experimental Mechanics, Spring Conference, Houston (1987) (to appear)  
(b) Proceedings of the Conference "Acousto-Ultrasonics: Theory and Applications," VPI & SU, Blacksburg, Virginia, July 1987, Eds: J.C. Duke and E.G. Henneke (to appear)  
(c) Proceedings of the 16th Symposium on Nondestructive Evaluation, San Antonio, Texas, April 1987 (to appear).
5. V.K. Kinra, "Dynamic Young's Modulus Measurements in Metallic Materials: Results of Interlaboratory Testing Program," Journal of Testing and Evaluation (authors: Wolfenden, Blessing, Chen, Dayal, Harmouche, Kinra, Liemmens, Phillips, Smith, Tetranova and Wann) (to appear).
6. V. Dayal and V.K. Kinra, "Nondestructive Evaluation of Fiber-Reinforced-Composites by Leaky Lamb Waves," Proceedings of Second International Conference on Testing, Evaluation and Quality Control of Composites (TEQC 87), University of Surrey, Guildford, England, September 1987 (to appear).
7. V.K. Kinra and V. Dayal, "A New Technique for Ultrasonic NDE of Thin Specimens," Experimental Mechanics, (accepted for publication).
8. V. Dayal, V.K. Kinra and J.G. Eden, "Nondestructive Testing of Matrix Cracks in Fiber-Reinforced Composites," Experimental Mechanics (to be submitted).
9. V. Dayal and V.K. Kinra, "Lamb Waves in Anisotropic Plates Immersed in a Fluid. An Exact Solution," Experimental Mechanics (to be submitted).
10. V. Dayal and V.K. Kinra, "Ultrasonic NDE of Composite-Materials Using Lamb Waves," Experimental Mechanics (to be submitted).
11. V.K. Kinra and V. Dayal, "Ultrasonic NDE of Fiber-Reinforced Composite Materials - A Review," to appear in the Proceedings of the International Conference on Composite Materials and Structures, Madras, India, January 1988.

#### 4. PROFESSIONAL PERSONNEL INFORMATION

1. Dr Vikram K. Kinra, Principal Investigator
2. Mr. J.G. Eden, M.S. (1985)
3. Mr. V. Dayal, Ph.D. (1987)
4. Mr. V. Iyer, Ph.D. (In progress)
5. Mr. C.Q. Rousseau, Undergraduate Research Assistant
6. Mr. R. Smith, Undergraduate Research Assistant
7. Mr. J. Grillo, Laboratory Technician - Mechanical
8. Mr. P. Patti, Laboratory Technician - Electronics
9. Ms. C. Rice, Secretary.